RIB-13

Subject Category: INSTRUMENTATION

UNITED STATES ATOMIC ENERGY COMMISSION

ELECTRONIC DEVICES FOR NUCLEAR PHYSICS

Quarterly Report No. 23 for February 1, 1956–April 30, 1956

By
M. H. Greenblatt
R. M. Matheson
A. H. Sommer
G. O. Fowler

June 15, 1956

David Sarnoff Research Center
Princeton, New Jersey

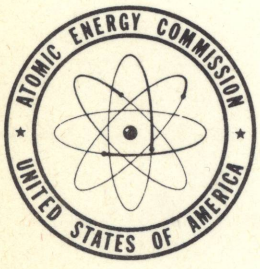

Technical Information Service Extension, Oak Ridge, Tenn.

This report has been reproduced directly from the best available copy.

Printed in USA, Price 25 cents. Available from the Office of Technical Services, Department of Commerce, Washington 25, D. C.

AEC, Oak Ridge, Tenn.

Quarterly Report No. 23

Contract W-7405-eng-26
Sub-308 *

ELECTRONIC DEVICES FOR NUCLEAR PHYSICS

(A report on photomultiplier tube development)
February 1, 1956 - April 30, 1956

June 15, 1956

Work on Contract done by:

M. H. Greenblatt
R. M. Matheson
A. H. Sommer
G. O. Fowler

Technical direction by:

G. A. Morton

This report also covers work on photoelectric emission which is not included in the contract, and was done by:

W. E. Spicer
A. H. Sommer

RCA LABORATORIES
DAVID SARNOFF RESEARCH CENTER
PRINCETON, N. J.

*Sponsored by the Special Electronics Development Program, Radiation Instruments Branch, U.S. Atomic Energy Commission, Washington, D. C. by subcontract through Oak Ridge National Laboratory.

PART I

MULTI-ALKALI PHOTOCATHODES

Work on multi-alkali cathode multipliers continued, in close cooperation with the RCA-Lancaster plant. Activation of the photocathode has proved to be reproducible without difficulty, but improved performance is still required in some respects.

With regard to thermionic emission from the cathode, it now appears certain that the Sb-K-Na-Cs cathode is as good as the conventional Sb-Cs cathode, with values in the range of 10^{-15} amps/cm and less. These figures have been confirmed by measurements in Lancaster.

However, dark currents of origins other than thermionic emission are still troublesome, particularly at inter-stage voltages exceeding 100 volts. Whereas in standard tubes with Sb-Cs activation sufficient gain is obtained with 100 volts per stage, the gain in multi-alkali tubes is somewhat lower and an inter-stage voltage of 150 volts would be desirable. There are several reasons for the lower gain in multi-alkali tubes; in the case of Ag-Mg dynodes, it has so far proved impossible to obtain with K-Na-Cs activation secondary emission factors as high as with Cs-activation alone, probably owing to a somewhat higher work function of the active surfaces. The alternative of alkali-metal-Sb dynodes has so far been

unsuccessful because the activation process of the photocathode is so critical that it has not yet been possible to combine it with a useful dynode activation process. In addition, by analogy with the results obtained with Ag-Mg dynodes, it is quite likely that the gain of an Sb dynode activated with K, Na and Cs is inferior to that of a standard Sb-Cs dynode. It should be emphasized that the loss in gain per stage is really quite small and is only appreciable in the total factor because of the large number of stages.

Work continues both on improving the gain of Ag-Mg dynodes and on developing a satisfactory activation process for Sb-dynodes. However, a more certain way of obtaining high overall gain consists of increasing the number of stages or the volts per stage. The first alternative is being tried now by preparing 14-stage tubes of the Type 6810 with multi-alkali cathodes. The second is at present hampered by the high dark currents at higher inter-stage voltages which were mentioned before.

These dark currents increase with voltage at a higher rate than the gain factor, indicating that they must be caused by either a gas effect or some sort of non-ohmic leakage. Several tubes were therefore made with an attached ion-gauge to investigate the first possibility. It was expected that if the dark current was due to excessive gas pressure, this would show up on the gauge, but no such effect was found.

The gauge was also run for long periods to act as an "ion pump" but again no significant effect on the dark current was observed.

It is, therefore, believed that the dark current is due to "non-ohmic" leaks, possibly associated with the chemical action of the alkali metals on the ceramics which are used as insulating supports in the multiplier. A tube in which the ceramic is replaced by glass is in preparation and it is hoped that with this change higher inter-stage voltages will become practicable.

II. Fundamental Studies of the Electronic Properties of Alkali Antimonide Compounds

Previous work has indicated that the alkali metals can be reacted with antimony to form compounds in the ratio of three alkali atoms per antimony atom. X-ray studies have indicated that the materials so formed are polycrystalline rather than amorphous and thus should exhibit energy band structure. It would seem of value to determine the band structure of any such a family of materials; however, the fact that these materials are also very efficient photoemitters is an added incentive. For, once such a determination is made, it is possible to study the photoemission in the view of the known band structure. This determination of the band structure is still in progress and the results to be reported here must be considered as somewhat preliminary in nature.

The problem has been approached by a study of the spectral distribution of the photoemission, photoconductivity, and optical absorption of very thin films of these materials. Fig. 1 illustrates the method by which the data is analyzed. This is simplicity itself. The threshold energy for photoconductivity and optical absorption would define the band gap, E_G; whereas, the threshold for photoemission, E_{PE}, would give the sum of electron affinity, E_A, and band gap, E_G. Therefore, the electron affinity would be given by

$$E_A = E_{PE} - E_G .$$

There are a number of assumptions inherent in such an interpretation; however, for brevity, these will not be discussed at this time. The difficulty in this method is in assigning values to these thresholds from the experimental curves.

Fig. 2 indicates typical curves obtained from Na_3Sb films. On the abscissa is plotted photon energy in ev (a scale in Angstrom units is given above the curves). On the lefthand ordinate is plotted the absorption $(1-I/I_o)$. On the righthand ordinate is plotted the logarithm of photoelectric yield in electrons/photon. Both the logarithm of photoconductivity (plotted to the same scale as the photoemission) and a linear plot of photoconductivity (normalized to the absorption at a certain indicated photon energy) are included in the figure.

All the films studied were very thin (probably being between 200 and 600 Å thick); thus, a few percent transmission would be expected for absorption coefficients of 10^6/cm or larger, i.e., for the maximum absorption coefficients in the fundamental region. As a result, it is possible to study the absorption in the fundamental region quite well, but the band edge does not show up at all sharply since there is only a few percent absorption in the region at which the band edge appears. This work is now being extended to thicker samples in the hope that the band edge may be made more distinct. However, this absorption in the fundamental region is, itself, of interest.

The absorption rises relatively slowly from 1.0 ev until reaching a maximum at about 2.8 ev; from 2.8 ev it decreases slightly with increasing $h\nu$.

Because of the lack of sharpness of the absorption cut off, it is necessary, at present, to define the band edge from the photoconductivity data. The band edge will be defined as 0.1 ev less than the energy at which the photoconductivity curves begin the steep exponential. Thus for Na_3Sb, a value of 1.0 ev is obtained for the band gap.

Likewise, the photoemissive threshold is defined as the energy at which the photoemissive efficiency has dropped to a value of 10^{-8} electrons/photon. As may be seen from the figures which follow, the photoemission drops much more steeply for the other alkali antimonides studied than for Na_3Sb. Using this convention for Na_3Sb, an affinity of 1.3 is obtained. Note that the photoelectric efficiency at 3.8 ev is about 1/2%.

The results obtained from K_3Sb are plotted in Fig. 3. The most striking thing about the absorption of this material is the dip at about 3.1 ev. This has appeared in all of the K_3Sb samples studied and seems very definitely to be a real effect. From the K_3Sb photoconductivity data, a band gap energy of 1.0 ev is obtained. From this and the photoemissive curve an electron affinity of about 0.7 ev is obtained. Note that with this reduction in electron affinity (compared to that of Na_3Sb) the photoemissive efficiency at 3.8 ev has increased from 1/2% to about 6%. The drop in efficiency past 3.8 ev is

probably due to the pyrex bulb used here.

Fig. 4 shows the data obtained for Rb_3Sb. From this a band gap of 1.1 ev and an electron affinity of 0.6 or 0.7 ev are estimated. The efficiency at 3.8 ev is about 7%. Note that the absorption here, as for all of the materials except K_3Sb, rises relatively slowly to a peak value and then tends to decrease.

In Fig. 5, typical data taken from Cs_3Sb is given. Here, the photoconductivity does not fit the absorption in the higher energy regions nearly as well as for the previously reported materials, nor does it break into the region of sharp exponential decay nearly as sharply as in these materials. This makes it somewhat more difficult to determine the band gap; however, it probably is between 1.0 and 1.2 ev. Combining this with the value for photoemissive threshold, an electron affinity between 0.4 and 0.6 ev is obtained. This cathode had an efficiency at 3.8 ev of about 13%.

Fig. 6 shows the data obtained from a multi-alkali cathode of the type Sb-K-Na. These cathodes have a very high dark conductivity at room temperature; thus, the photoconductivity could only be obtained by cooling the cathode to liquid nitrogen temperature. From this data, a band gap of about 1.0 ev is obtained. The affinity seems to be about 0.6 ev. The efficiency at 3.8 ev is about 20%. It has been found in the past that by adding what appears to be a cesium monolayer to a Sb-K-Na cathode, the photoelectric threshold can be moved

a considerable distance farther into the infrared, but that this treatment does not change the absorption; the photoelectric threshold, however, is moved to 1.2 ev indicating an affinity of something like 0.2 ev. Thus the affinity is reduced by about 0.4 ev by the addition of the cesium. Although this treatment decreases the threshold energy, it does not seem to affect the photoelectric efficiency.

PART II

PHOTOMULTIPLIER DEVELOPMENT

I. Multiplier Structure with Improved Time Resolution

Design of the multiplying structure for a fast high-gain photomultiplier having a space-charge limited output current over 1 amp, utilizing central accelerating electrodes at a common high potential, and having a transit time dispersion substantially less than 3×10^{-9} sec. is reported.

The work so far completed includes extensive rubber model trajectory plotting, the construction of a small resistance network analog, numerical improvement of the field by iteration and "over-correction," superposition of the several field components, a numerical trajectory calculation, construction and testing of a large scale-model tube.

The results of the trajectory calculations are shown in Fig. 7. These trajectories have been determined for a central electrode potential of 5000 volts, and potentials of 700 and 800 volts for the emitting and receiving dynodes, respectively. Comparison of the calculated results shown in the figure with the trajectories obtained with the rubber model (see Fig. 6, Quarterly Report No. 20) indicates substantial agreement in the trajectories obtained by the two methods. In particular, it shows that the energy loss which was expected to vitiate rubber model results close to the surface of the receiving dynode is considerably smaller than was anticipated.

The large scale-model tube consists of a five-stage multiplier of about four times the linear scale of the proposed final structure. The electron source is an electron gun, and deflection of the spot on the first dynode serves to display the focusing behavior at the phosphor-coated second, and succeeding, dynodes. A drawing of this structure is shown in Fig. 1 of Report No. 22. A photograph of the completed tube is shown in Fig. 8.

Direct visual observation of the impact points of electrons both on the dynodes and on the lateral supporting micas in this tube as well as measurements of currents to the various electrodes confirm the results obtained by calculation and from the rubber model.

These calculations and observations tend to confirm the discussion of the design problems set forth in Report No. 20, and indicate that the bilateral symmetry of electron velocity about the central plane imposes very severe restrictions on the choice of multiplier geometry.

II. Time Resolution of Photocathode-First Dynode System

Time resolution measurements made at the University of California by Kerns, Kirstan and others on the Type 6810 photomultiplier indicate that the time spread in the photocathode-first dynode system of these tubes is a major limiting factor. A time difference of six to eight millimicroseconds is observed in electrons leaving from the center of the cathode as compared with those leaving from the edge. This is to be compared with the transit time spread in the structure itself which is about 1.5 millimicroseconds. If the time spread in the cathode region could be eliminated in this tube type, the performance would be improved by a factor of at least five.

Initially it had been planned to complete the design of the high-speed structure described in the previous section before undertaking the design of an improved cathode-to-first dynode system. However, the obvious need for an improved system makes it evident that at least a partial solution to this second problem should be worked out before completing the structure. Obviously, the problem of good time resolution between the photocathode and first dynode cannot be wholly divorced from that of the efficient collection of photoelectrons. A satisfactory solution from the time standpoint must also be one in which electrons are collected from all portions of the cathode with reasonably high efficiency. To effect the required improvement, three different lines

of approach are being explored, namely, equalization of path lengths, improvement of the field distribution and the use of higher potentials and consequently greater field strengths in the cathode region.

Estimates made of the transit times of a few typical trajectories through this region of a Type 6810 photomultiplier show that one of the major contributing factors is the difference in path lengths between center and edge of the photocathode. The simplest configuration giving equal paths is one where the cathode is a spherical surface with a small first dynode located at its center of curvature. This solution is not, however, from a practical standpoint the optimum. If the distance between the cathode and first dynode is small, the cathode must have considerable curvature which introduces optical problems when the multiplier is used for scintillation counting. If, on the other hand, the cathode to first dynode distance is made large to reduce the curvature of the cathode, the time spread due to differences in initial velocities is accentuated. Also, this solution involves rather complicated distribution of potentials along the boundaries of the cathode to first dynode region in order to simulate the spherical geometry. Fig. 9 shows schematically possible forms for such an electron collector system.

The field distribution in the volume between the cathode and first dynode also has an important bearing on the transit time of electrons leaving different points of the cathode. Fig. 10 is an imaginary electrode configuration and

potential distribution which illustrates the principal here involved. An electron leaving point "a" at the center of the cathode is accelerated rather slowly out to the surface LL' which is an electron lens. An electron leaving point "b" near the edge of the cathode is accelerated by a rather strong field and moves through most of the distance to LL' at or near its maximum velocity. The lens LL' focuses both electrons to point "0" on the first dynode. The electron from point "a" has a shorter distance to travel than does the electron from "b". However, this difference in distance is compensated for by the fact that it reaches the surface LL' later than does the electron from "b".

The actual configuration used will employ both of these ways of obtaining isochronous trajectories. Also, the system will be designed in such a way that the aperture disk or its equivalent which separates the cathode volume from the rest of the multiplier is operated at a fairly high potential, higher even than that of the first dynode. This, in turn, reduces the effect of both initial velocities and path differences.

Because these systems are cylindrically symmetrical the rubber model cannot be employed. It will be necessary to plot potential distributions with the aid of the resistance network analog and then to solve for electron trajectories. Test multipliers will be built and their time performance

measured to compare with the calculated results. Time measuring equipment patterned after that used at the University of California will be constructed in order to carry out these measurements.

III. Time Resolution Measurements of Multiplier Structures

Transit time spread measurements on the DuMont type multiplier structure were completed. This was done using the equipment developed for measuring time spread in any multiplier structure. The unit employs a short electron pulse generated by sweeping a beam across an aperture. The time distribution of the electrons corresponding to the multiplied pulse from the structure being tested is analyzed by forming it into a beam and sweeping it across a probe electrode.

Measurements on tube No. 6791-5 containing the DuMont dynode system could not be made at 50 mc, the frequency used for testing the 6810 and the 931-A structures. It was found necessary to reduce the frequency to 5 mc before a satisfactory measurement could be obtained, Fig. 11 shows the results obtained with this tube at 5 mc. It will be seen that the pulse output of the multiplier is not less than 20 millimicroseconds duration, This is the transit time dispersion for the 6-stage structure used. The transit time spread per dynode is, therefore, approximately 8 to 10 millimicroseconds. Included in Fig. 11 is the data taken with tube No. 6791-3 (containing the L-16 dynode structure) taken at 5 mc. It will be apparent that the transit time dispersion of this tube cannot be measured at the low frequency.

Transit time dispersion measurements have now been put on a fairly routine basis. One more structure, namely,

the H-5723 is to be measured to complete the measurements of transit time spread for existing multipliers. Work with this equipment will then be suspended until the higher speed structure mentioned in Section I is developed. A paper is being prepared describing these time measurements.

IV. Miscellaneous

In order to simplify testing of multipliers where it is desired to change the potential on individual dynodes, a high voltage supply was built which takes the form of a constant current generator. With this type of power supply, variable resistors can be used in the bleeder and changing the value of the resistor on one stage changes the voltage on that stage alone without effecting the voltage on the other stages. While this is not a new technique, it has not been widely used in the past. It is mentioned here because of its convenience. The constant current generator for this purpose is shown in the circuit diagram in Fig. 12. The current can be controlled over the range 1 to 5 milliamps and is regulated. The power supply is capable of a total voltage of 2000 volts.

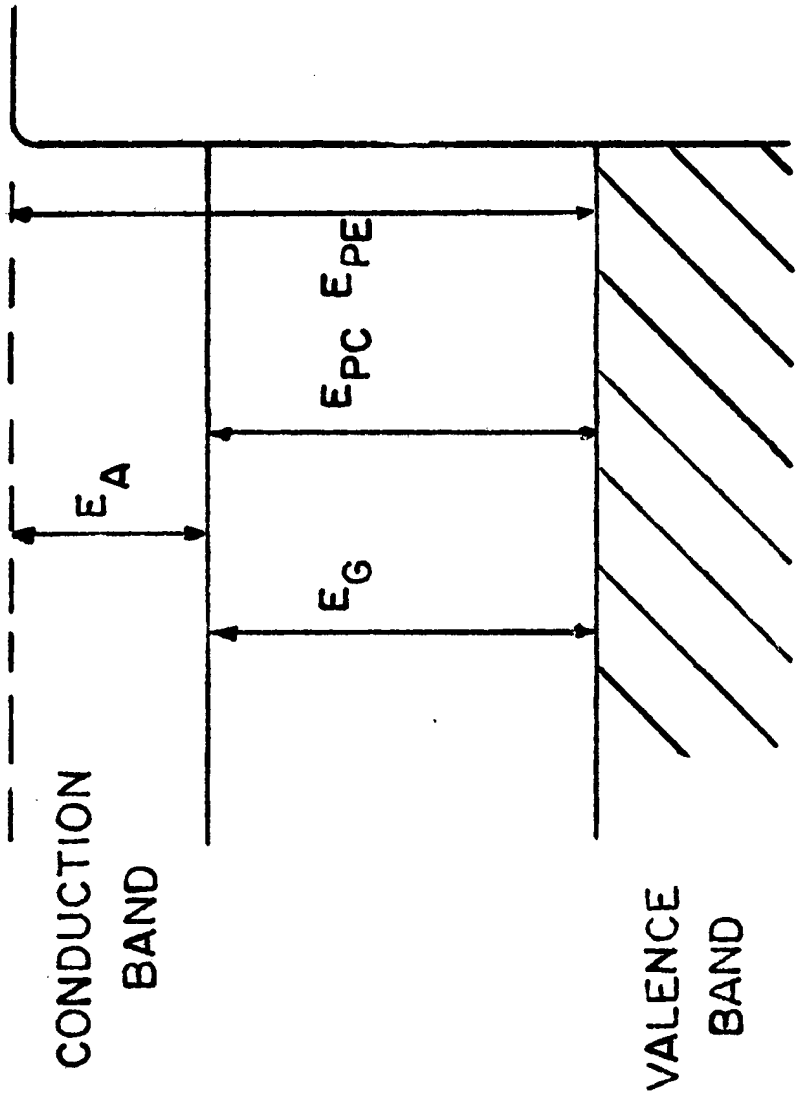

$E_G = E_{PC}$

$E_A = E_{PE} - E_{PC}$

Fig. 1

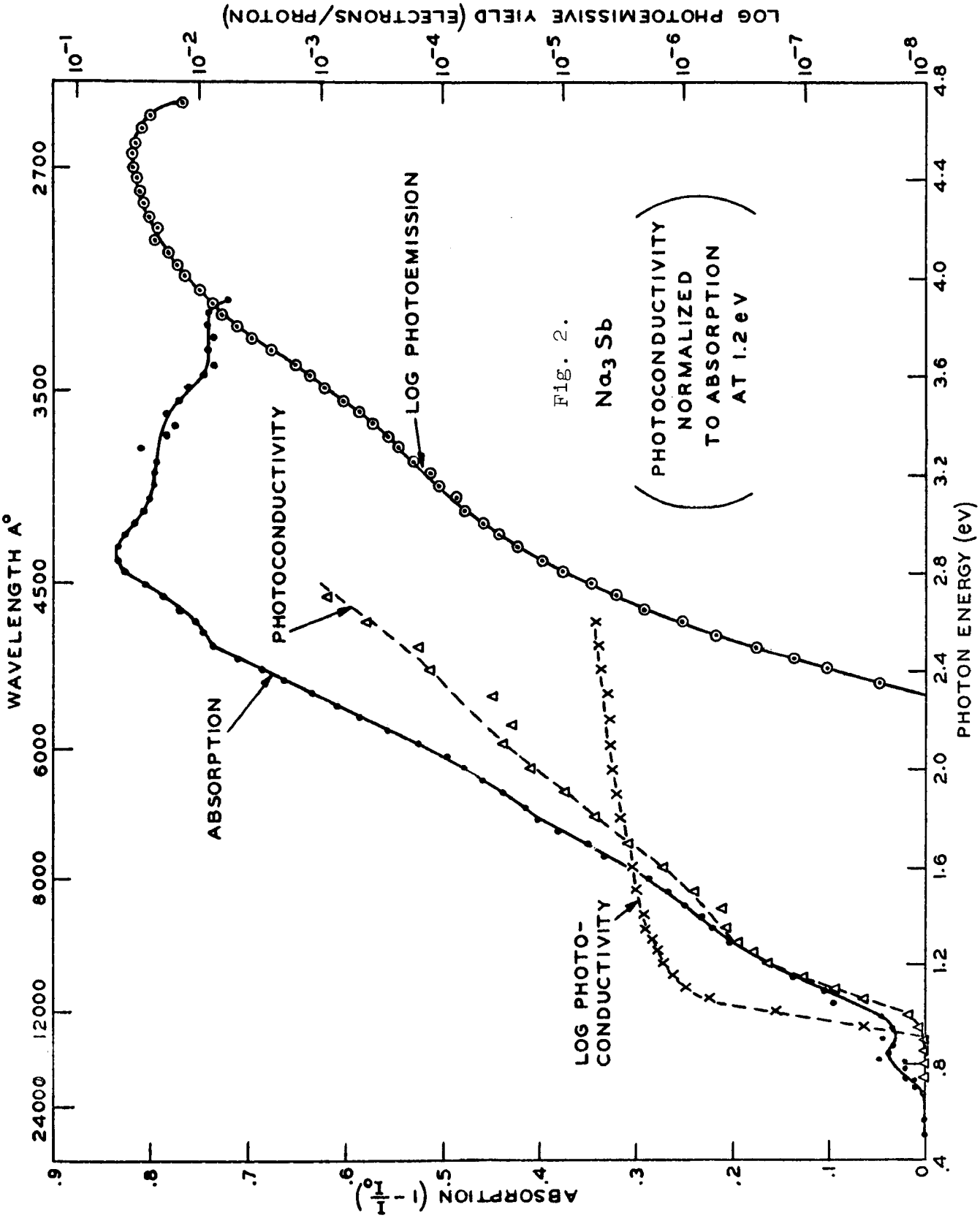
LOG PHOTOEMISSIVE YIELD (ELECTRONS/PROTON)
WAVELENGTH A°
PHOTON ENERGY (eV)
ABSORPTION $(1-\frac{I}{I_0})$
LOG PHOTOEMISSION
PHOTOCONDUCTIVITY
ABSORPTION
LOG PHOTO-CONDUCTIVITY
PHOTOCONDUCTIVITY NORMALIZED TO ABSORPTION AT 1.2 eV
Na_3Sb

Fig. 2.

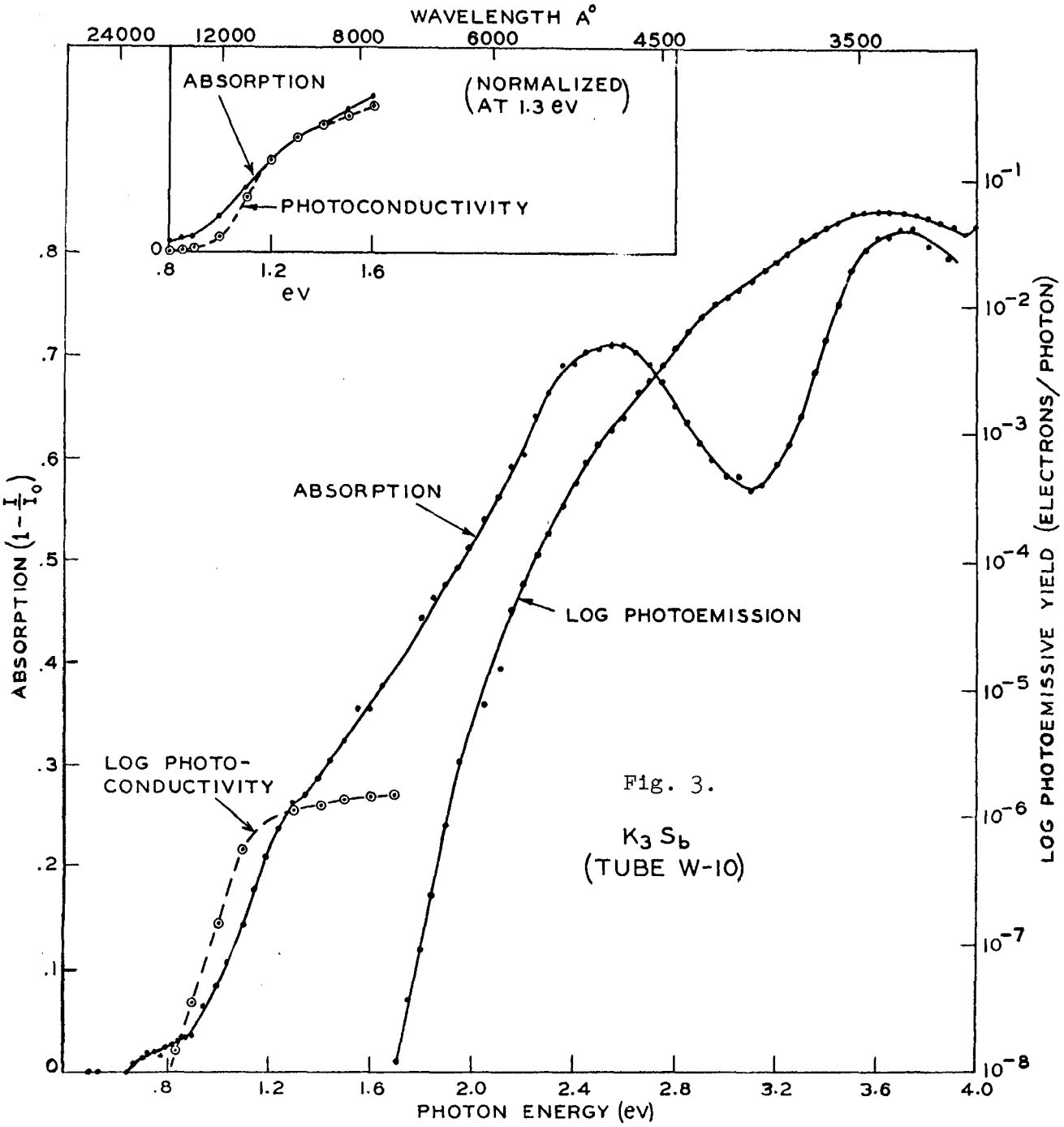
WAVELENGTH A°
24000
12000
8000
6000
4500
3500
ABSORPTION
(NORMALIZED AT 1.3 eV)
PHOTOCONDUCTIVITY
0
.8
1.2
1.6
eV
ABSORPTION (1 - I/I0)
ABSORPTION
LOG PHOTOEMISSION
LOG PHOTO-CONDUCTIVITY
LOG PHOTOEMISSIVE YIELD (ELECTRONS/PHOTON)
PHOTON ENERGY (eV)
K3 Sb
(TUBE W-10)

Fig. 3.

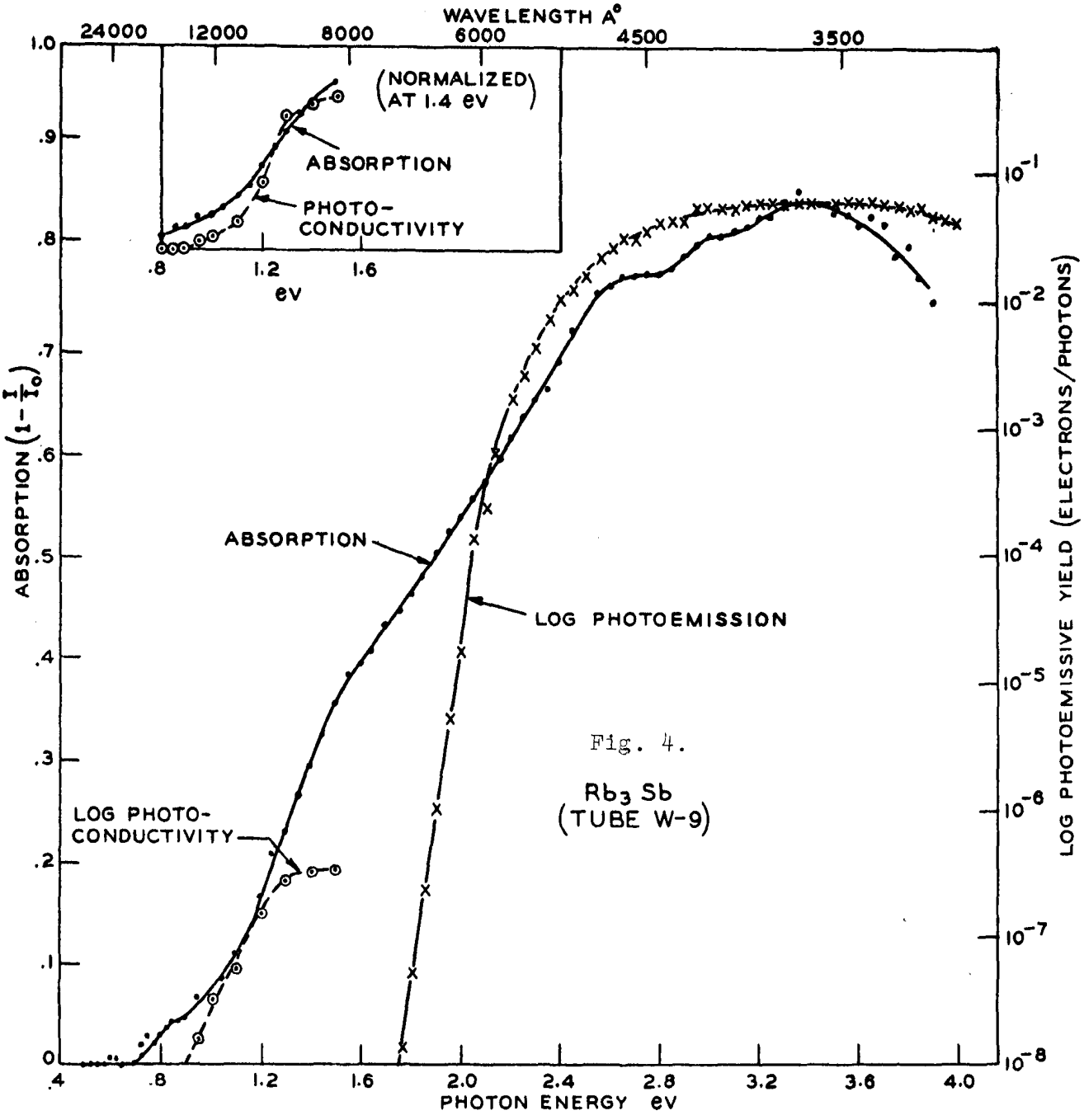

Fig. 4.

Rb_3Sb
(TUBE W-9)

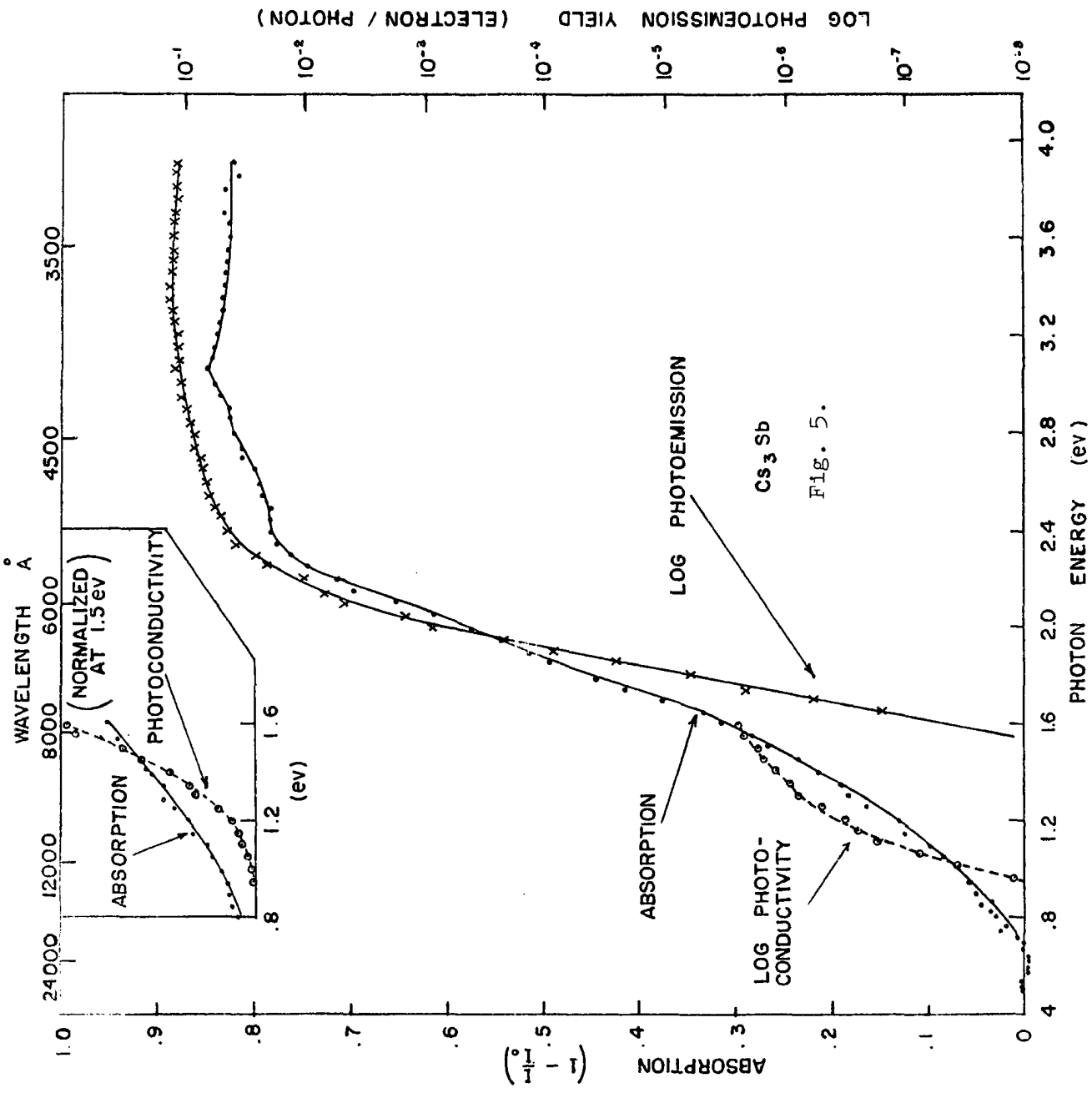
WAVELENGTH Å
24000
12000
8000
6000
4500
3500
1.0
.9
.8
.7
.6
.5
.4
.3
.2
.1
0
ABSORPTION $\left(1 - \frac{I}{I_0}\right)$
LOG PHOTOEMISSION YIELD (ELECTRON / PHOTON)
10^{-1}
10^{-2}
10^{-3}
10^{-4}
10^{-5}
10^{-6}
10^{-7}
10^{-8}
4
.8
1.2
1.6
2.0
2.4
2.8
3.2
3.6
4.0
PHOTON ENERGY (ev)
LOG PHOTOEMISSION
Cs_3Sb
ABSORPTION
LOG PHOTO-CONDUCTIVITY
ABSORPTION
PHOTOCONDUCTIVITY
(NORMALIZED AT 1.5 ev)
.8
1.2
1.6
(ev)

Fig. 5.

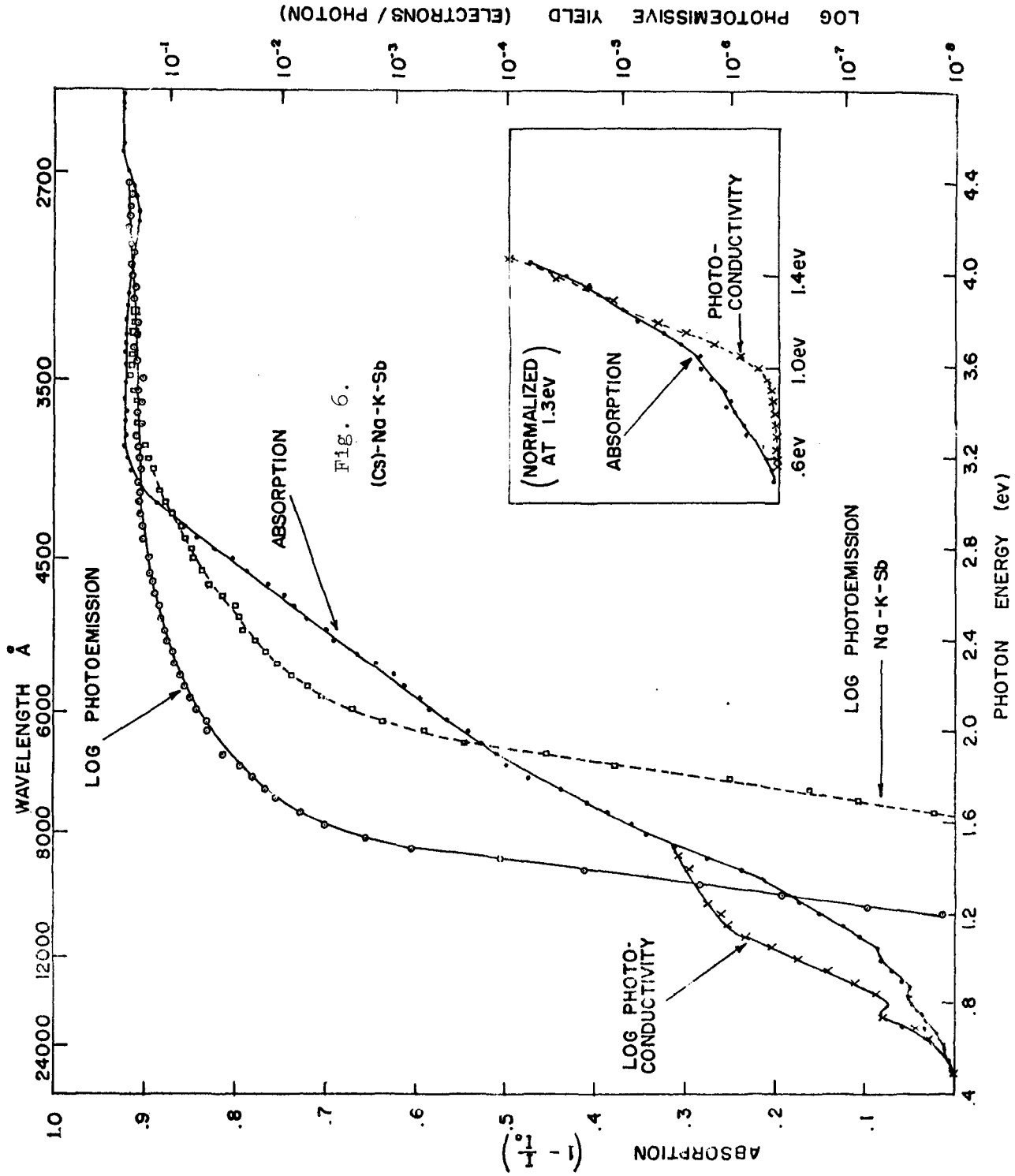
WAVELENGTH Å
24000
12000
8000
6000
4500
3500
2700
PHOTON ENERGY (eV)
1.2
1.6
2.0
2.4
2.8
3.2
3.6
4.0
4.4
ABSORPTION
LOG PHOTOEMISSIVE YIELD (ELECTRONS / PHOTON)
LOG PHOTOEMISSION
LOG PHOTOCONDUCTIVITY
ABSORPTION
(Cs)-Na-K-Sb
LOG PHOTOEMISSION
Na-K-Sb
(NORMALIZED AT 1.3eV)
ABSORPTION
PHOTO-CONDUCTIVITY
.6ev
1.0ev
1.4ev

Fig. 6.

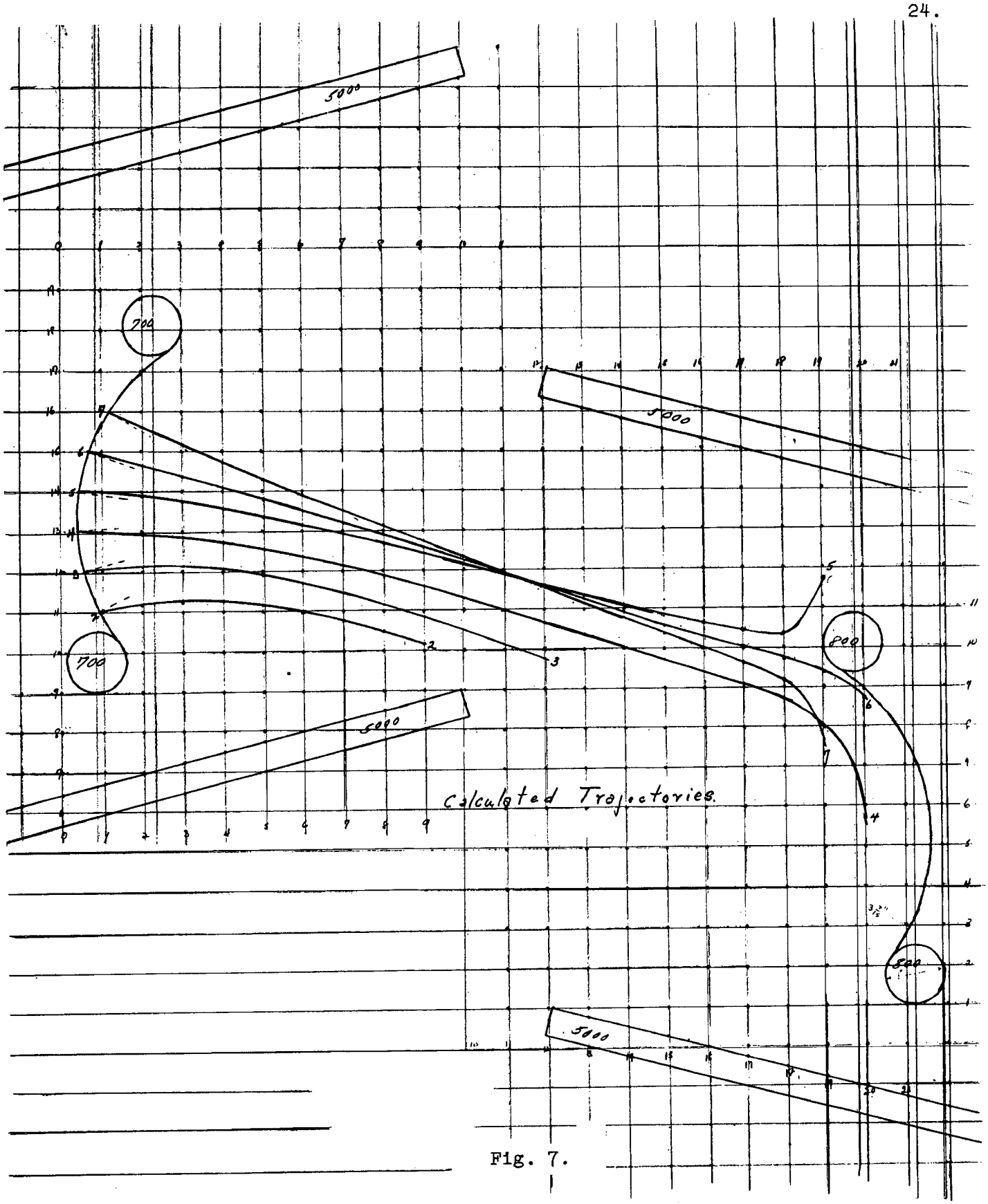
5000
700
5000
700
800
5000
800
5000
Calculated Trajectories.

Fig. 7.

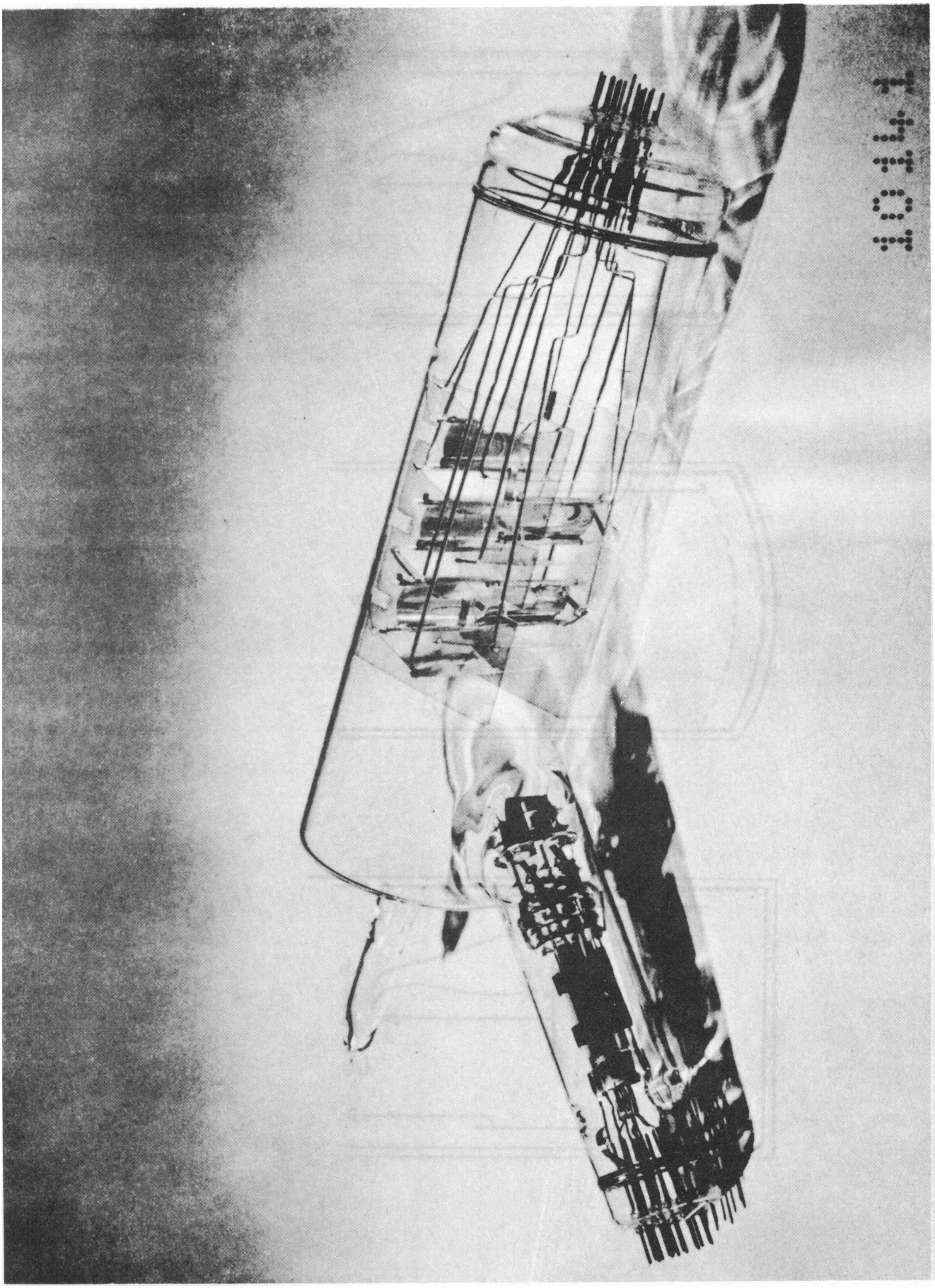

Fig. 8. Large Scale-Model Central Potential Multiplier

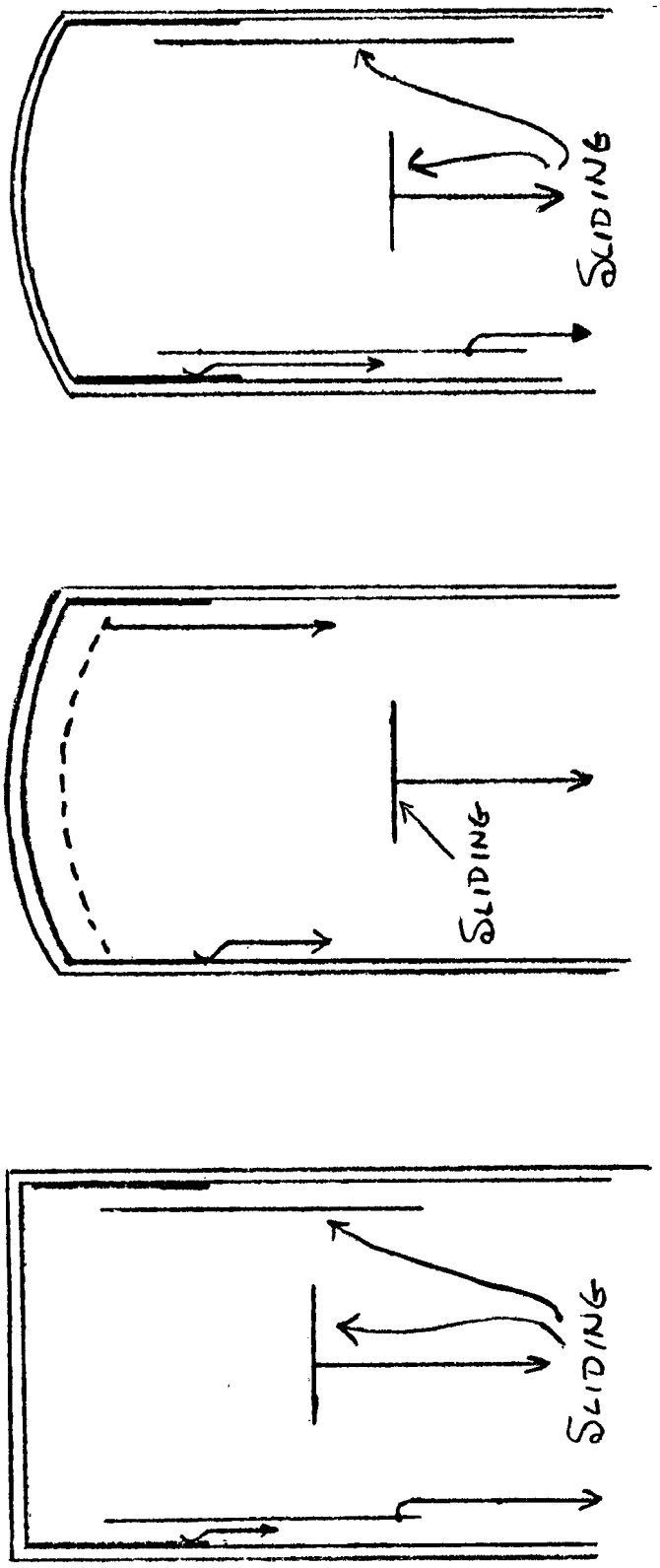

Fig. 9

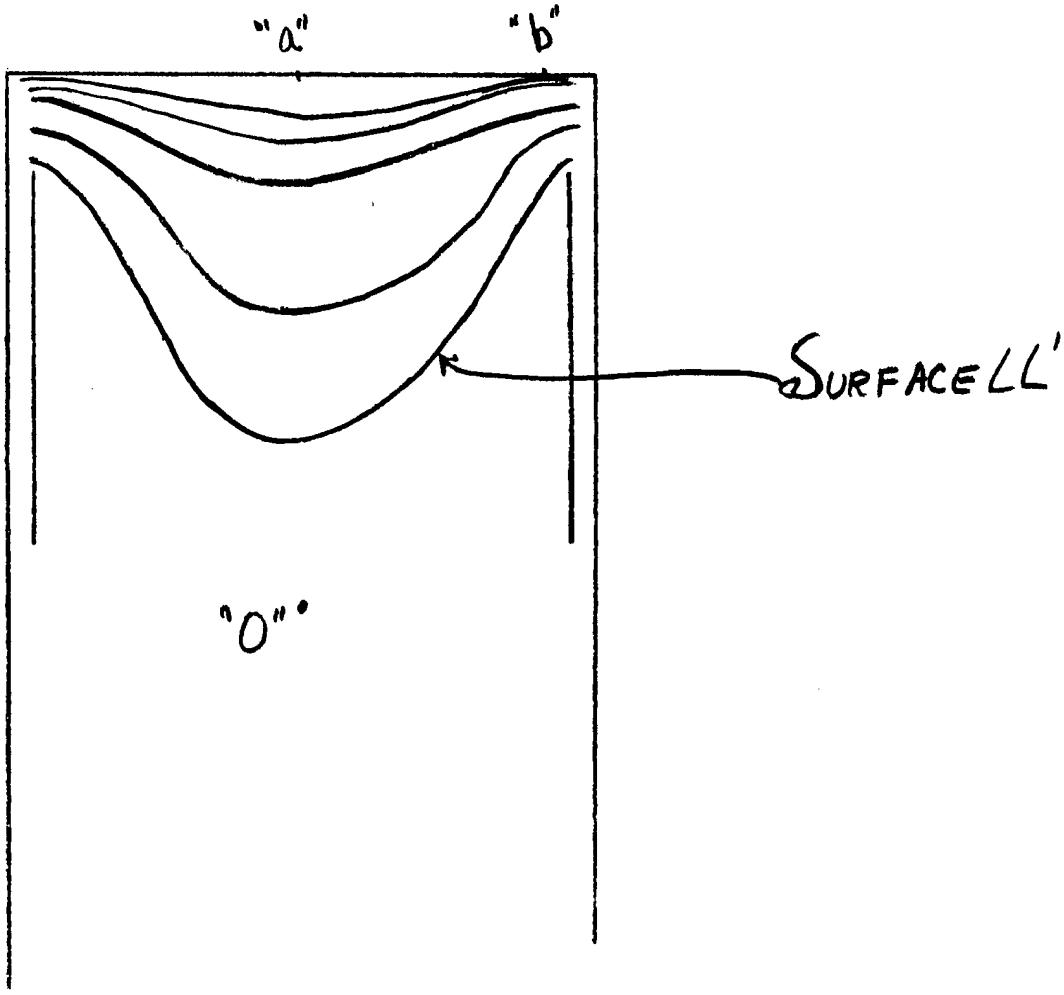

Fig. 10.

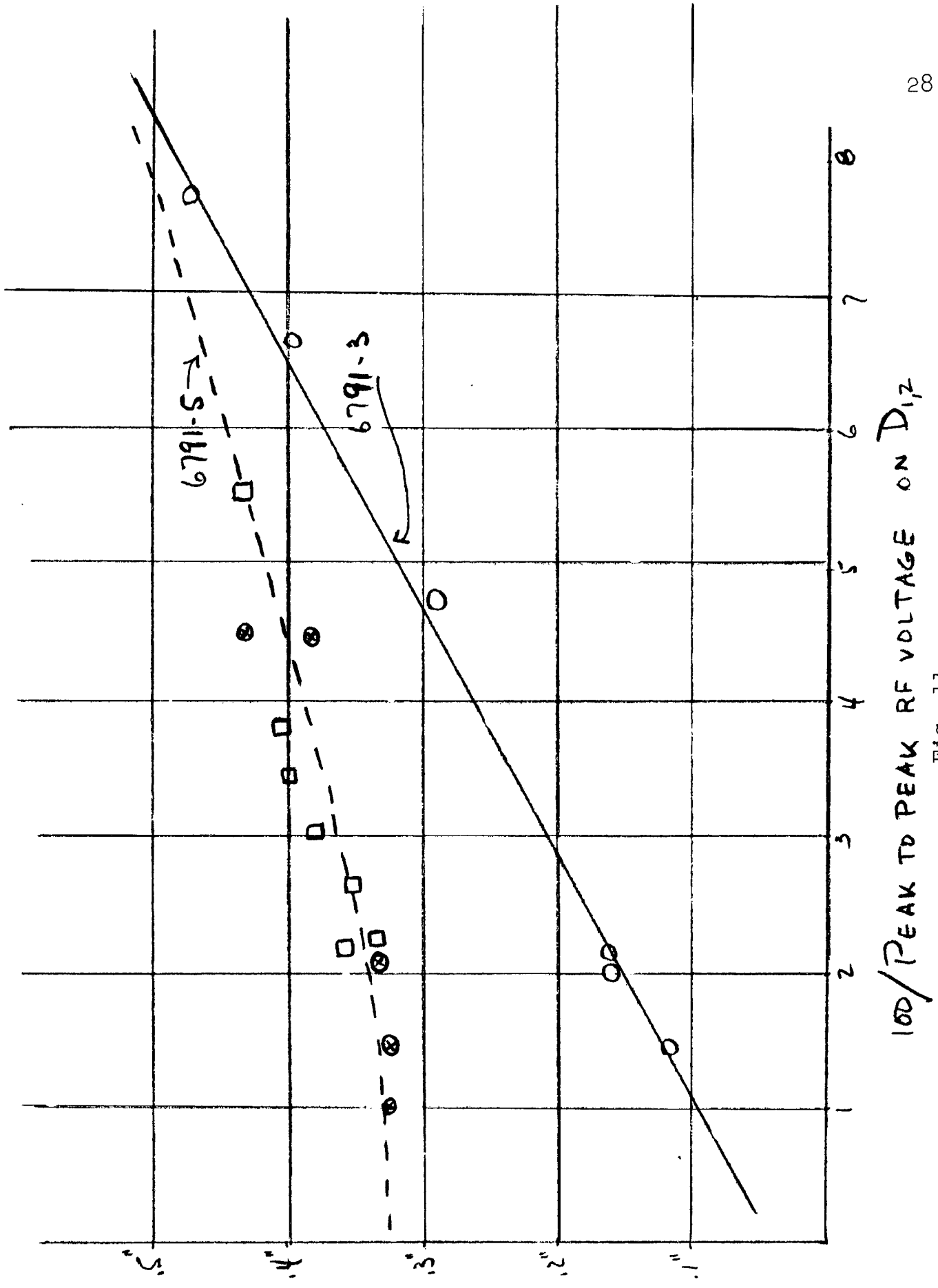
WIDTH OF OUTPUT PULSE (0.10⁻⁹ SEC/i" AT 5 d/MC)
1
2
3
4
5
6
7
8
1D/PEAK TO PEAK RF VOLTAGE ON D1,2
6791-5
6791-3

Fig. 11.

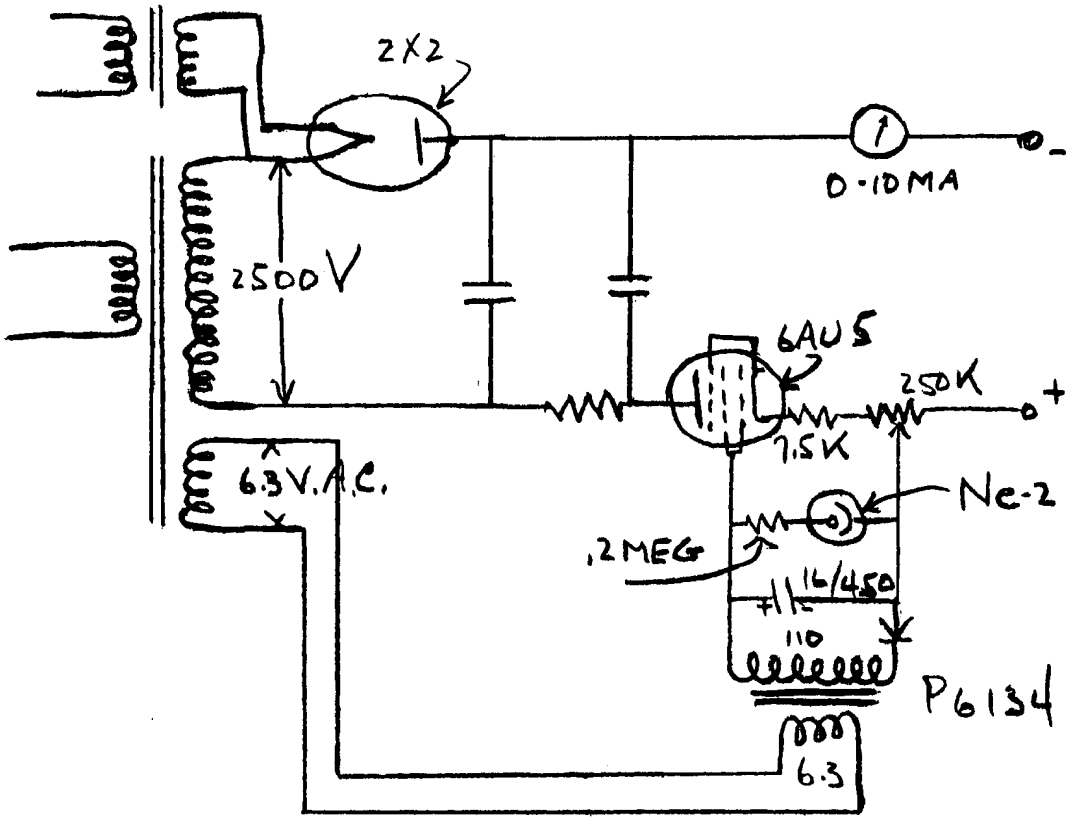
2X2
0-10MA
2500V
6AU5
250K
7.5K
6.3V.A.C.
Ne-2
.2MEG
16/450
110
P6134
6.3

Fig. 12